CJC Pediatric and Congenital Heart Disease 2 (2023) 12–19

Original Article

# Automatic Prediction of Paediatric Cardiac Output From Echocardiograms Using Deep Learning Models

Steven Ufkes, MSc,[a] Mael Zuercher, MD,[b,c] Lauren Erdman, MSc,[a] Cameron Slorach, RDCS,[d,*] Luc Mertens, MD, PhD,[d,f] and Katherine L. Taylor, BMed, PhD, FANZCA[b,e]

[a] *Division of Genetics and Genome Biology, Centre for Computational Medicine, The Hospital for Sick Children, Research Institute, Toronto, Ontario, Canada*

[b] *Department of Anesthesia and Pain Medicine, The Hospital for Sick Children, Toronto, Ontario, Canada*

[c] *Department of Anesthesia, Centre hospitalier universitaire Vaudois, Lausanne, Switzerland*

[d] *Department of Cardiology, The Hospital for Sick Children, Toronto, Ontario, Canada*

[e] *Department of Anesthesia, University of Toronto, Toronto, Ontario, Canada*

[f] *Department of Pediatrics, University of Toronto, Toronto, Ontario, Canada*

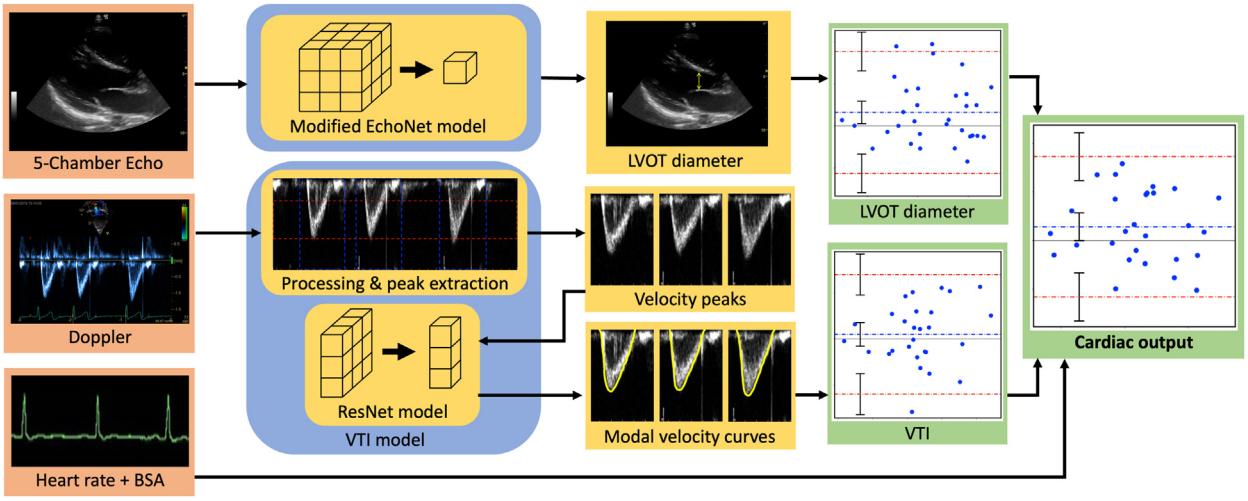


## ABSTRACT

**Background:** Cardiac output (CO) perturbations are common and cause significant morbidity and mortality. Accurate CO assessment is crucial for guiding treatment in anaesthesia and critical care, but

## RÉSUMÉ

**Contexte :** Les perturbations du débit cardiaque sont fréquentes et associées à des taux élevés de morbidité et de mortalité. Une évaluation juste du débit cardiaque est essentielle pour orienter le

Cardiac output (CO) determines tissue oxygen delivery and can change rapidly during anaesthesia and surgery. In anaesthesia and critical care, CO assessments guide therapeutic decision-making and responses to treatment. CO assessment by clinical examination is difficult, even for experienced clinicians, especially in the early stages of deterioration.[1] Registry data show that 67% of anaesthesia-related paediatric cardiac

Received for publication September 12, 2022. Accepted November 3, 2022.

*This author has now retired.

Corresponding author: Dr Katherine Taylor, Department of Anesthesia and Pain Medicine, the Hospital for Sick Children, 555 University Ave, Toronto, Ontario M5G 1X8, Canada. Tel.: +1-416-442-6154.

E-mail: Katherine.taylor@sickkids.ca

https://doi.org/10.1016/j.cjcpc.2022.11.001

**measurement is difficult, even for experts. Artificial intelligence methods show promise as alternatives for accurate, rapid CO assessment.**

**Methods:** **We reviewed paediatric echocardiograms with normal CO and a dilated cardiomyopathy patient group with reduced CO. Experts measured the left ventricular outflow tract diameter, velocity time integral, CO, and cardiac index (CI). EchoNet-Dynamic is a deep learning model for estimation of ejection fraction in adults. We modified this model to predict the left ventricular outflow tract diameter and retrained it on paediatric data. We developed a novel deep learning approach for velocity time integral estimation. The combined models enable automatic prediction of CO. We evaluated the models against expert measurements. Primary outcomes were root-mean-squared error, mean absolute error, mean average percentage error, and coefficient of determination ($R^2$).**

**Results:** **In a test set unused during training, CI was estimated with the root-mean-squared error of 0.389 L/min/m$^2$, mean absolute error of 0.321 L/min/m$^2$, mean average percentage error of 10.8%, and $R^2$ of 0.755. The Bland-Altman analysis showed that the models estimated CI with a bias of +0.14 L/min/m$^2$ and 95% limits of agreement -0.58 to 0.86 L/min/m$^2$.**

**Conclusions:** **Our model estimated CO with strong correlation to ground truth and a bias of 0.17 L/min, better than many CO measurements in paediatrics. Model pretraining enabled accurate estimation despite a small dataset. Potential uses include supporting clinicians in real-time bedside calculation of CO, identification of low-CO states, and treatment responses.**

**choix du traitement anesthésique et des soins critiques. Or, il est difficile de mesurer le débit cardiaque, même pour les experts. Les méthodes fondées sur l'intelligence artificielle semblent toutefois prometteuses pour évaluer le débit cardiaque avec exactitude et rapidité.**

**Méthodologie :** **Nous avons analysé des échocardiogrammes pédiatriques chez des personnes dont le débit cardiaque est normal ainsi que chez des patients qui étaient atteints d'une cardiomyopathie dilatée et dont le débit cardiaque était réduit. Des experts ont mesuré le diamètre de la voie d'éjection ventriculaire gauche, l'intégrale de la vitesse par rapport au temps (IVT), le débit cardiaque et l'index cardiaque. L'outil EchoNet-Dynamic est un modèle d'apprentissage profond qui donne une estimation de la fraction d'éjection chez les adultes. Nous avons modifié ce modèle afin qu'il puisse prédire le diamètre de la voie d'éjection ventriculaire gauche et l'avons entraîné à l'aide de données pédiatriques. Nous avons également mis au point une nouvelle approche d'apprentissage profond pour l'estimation des valeurs d'IVT. La combinaison de ces modèles a permis de prédire de façon automatique le débit cardiaque, et nous avons évalué les résultats obtenus par rapport à ceux des experts. Les principaux critères d'évaluation étaient l'erreur moyenne quadratique (EMQ), l'erreur moyenne absolue (EMA), le pourcentage d'erreur moyen (PEM) ainsi que le coefficient de détermination ($R^2$).**

**Résultats :** **Dans un ensemble d'essais n'ayant pas été utilisé au cours de l'entraînement du modèle, l'index cardiaque a été estimé avec une EMQ de 0,389 L/min/m$^2$, une EMA de 0,321 L/min/m$^2$, un PEM de 10,8 % et un $R^2$ de 0,755. Selon l'analyse de Bland-Altman, le biais pour les estimations de l'index cardiaque était de + 0,14 L/min/m$^2$, et les limites de concordance à 95 % étaient de −0,58 à 0,86 L/min/m$^2$.**

**Conclusions :** **Les estimations générées par le modèle pour le débit cardiaque montraient une forte corrélation avec les valeurs de référence et un biais à 0,17 L/min, ce qui est mieux que bien des mesures du débit cardiaque utilisées en pédiatrie. Malgré un petit ensemble de données, le modèle entraîné a permis de produire une estimation juste. Les utilisations potentielles comprennent l'aide aux cliniciens dans le calcul du débit cardiaque en temps réel et au chevet du patient, le dépistage d'un faible débit cardiaque et l'évaluation de la réponse au traitement.**

arrests are related to underestimating CO, inappropriately treating low-CO states, or medication-related low-CO states.[2,3] Early reversal of low-CO states improves outcomes in adult, paediatric and neonatal sepsis, adult high-risk surgery, vascular surgery, and trauma.[4–6] Incorrect, inadequate, or excessive treatment with vasopressors or inotropic agents can worsen CO.

A common indication of inadequate CO is hypotension, which may be due to decreased preload, systemic vasodilation, or decreased cardiac function. In paediatrics, fluid administration is a mainstay of haemodynamic resuscitation and CO augmentation, although not all children respond to fluid, and excess fluid administration can be harmful.[7,8] Excess fluid administration increases endothelial permeability,[8] delays wound healing, impairs respiratory function parameters,[9] and is an independent predictor of death in critically ill children and adults.[10,11] Dynamic variables of heart-lung interactions are good predictors of fluid responsiveness in adults, but not children.[12] Aortic blood flow peak velocity[12] and stroke volume index[13] have been shown to predict fluid responsiveness in children, but acquiring and interpreting these measurements is difficult and prone to error.

Many noninvasive CO measuring systems are available, but few are validated in paediatrics[14,15] or sufficiently accurate,[16,17] despite the acceptable mean percentage error of ± 30%.[18] Echocardiography is recognized as the clinical gold standard for measuring CO, and the superior haemodynamic monitor in critically ill paediatrics.[19,20] Noncardiologists are availing themselves of the increased availability of point-of-care ultrasound machines to perform focused echocardiography (FoCUS) to guide management of low-CO states. Paediatric image acquisition and interpretation can be challenging.

EchoNet-Dynamic[21] is a deep-learning algorithm trained on adult echocardiograms to calculate ejection fraction. In this study, we modified EchoNet-Dynamic to predict a different metric, left ventricular outflow tract (LVOT) diameter, from videos acquired in a different view than the original model and retrained it on paediatric data. We developed a novel deep-learning approach for the estimation of velocity time integral (VTI). The combination of these models enables

automatic estimation of CO. Our model estimated CO in a collection of anatomically normal paediatric echocardiograms with normal and reduced CO, within clinically acceptable diagnostic accuracy.

Deep-learning models are trained by example, repeatedly adjusting model parameters to better fit the data. This learning process is controlled by fixed hyperparameters, whose values can greatly affect the accuracy of the trained model.

## Methods

After research ethics board approval and waiver of consent, we identified a convenience sample of echocardiograms of children (1 day to 18 years old, 260 in total, acquired between 2005 and 2020) with normal cardiac anatomy or haemodynamically insignificant anomalies (e.g., patent foramen ovale and small atrial septal defect). Echocardiograms were chosen from a healthy population with normal CO and a group with dilated cardiomyopathy with reduced CO. Subject characteristics are given in Table 1. Echocardiograms were acquired on General Electric Vivid7, Vivid E9, and Vivid E95 (GE HealthCare, Waukesha, WI) by expert sonographers (C.S. and L.M.).

### Measurement of the LVOT diameter and VTI

The LVOT diameter was measured in a parasternal long-axis view within 0.5 cm of the aortic annulus at mid-systole by 2 investigators (C.S. and M.Z.). Either 1 or 2 cardiac cycles were examined, within which 3 measurements were made. The average was taken as the ground truth LVOT diameter and used to calculate the LVOT cross-sectional area ($CSA = \pi^*(d/2)^2$). The LVOT VTI measurements were calculated from an apical 5-chamber view (5Ch) using a pulse wave Doppler across the LVOT sampled immediately below the aortic valve. An expert sonographer (C.S.) selected and traced 2 or 3 typical velocity peaks in every Doppler image, and VTI was calculated as the average of the areas under the curves. To evaluate inter-rater reliability of VTI measurement, a second expert rater (M.Z.) evaluated VTI in a subset of these images. Heart rate was measured at the time of the Doppler ultrasound. CO was calculated as the product of LVOT CSA, LVOT VTI, and heart rate. We present CO results in terms of cardiac index (CI), defined as CO divided by body surface area estimated using the Haycock formula.

### Machine learning model

We designed a 2-part model for the calculation of CO from 5Ch echocardiography videos and pulse wave Doppler images. First, a deep-learning approach was used to calculate the LVOT diameter from 5Ch video. Secondly, a deep-learning approach was used to trace modal velocity curves in Doppler images, the areas under which were used to estimate VTI. All models were built using the Python library PyTorch.

Each subject was randomly assigned to 1 of 3 groups: 75% to a training set, whose data were used to train the models; 12.5% to a validation set, whose data were used to select parameters for the final models but not used to train models directly; and 12.5% to a test set, whose data were used for validation after all trained models were finalized. The numbers of subjects with each image type in each group are summarized in Table 1. Every available 5Ch video and Doppler image were used in its corresponding model. The subjects included in the CO model were those with both 5Ch video and Doppler images. Subject characteristics and cardiac metrics were compared between the 3 groups using analysis of variance.

### LVOT diameter calculation

To calculate the LVOT diameter from 5Ch videos, we modified the EchoNet-Dynamic deep-learning model, which was originally trained to calculate the left ventricular ejection fraction from 4-chamber apical view echocardiogram videos of 10,030 adults.[21] The EchoNet-Dynamic model consists of a sequence of 5 R(2+1)D convolutional blocks.[22] Each block performs 2D convolutions in space to extract and generate maps of spatial image features, followed by 1D convolutions in time, which extract temporal features. By composing spatial and temporal image features detected in previous blocks, successive blocks detect increasingly complex features. The convolutional blocks are followed by a pooling layer, which reduces the resolution of the feature maps. Finally, a fully connected layer combines the spatial and temporal features to output an estimation of the LVOT diameter.

Before being input to the model, 5Ch videos were preprocessed by the same procedure as the EchoNet dataset; videos were cropped around the scan region, converted to AVI, and normalized by subtracting the mean and dividing by the standard deviation of the videos in the training set.

The model was trained to minimize the mean squared error (MSE) between the estimated and actual LVOT diameter values using the Adam algorithm.[23] Training hyperparameters were selected by sequential model-based optimization using tree-structured Parzen estimators.[24] Additional details of the training procedure are given in the Supplemental Materials.

### VTI calculation

To estimate VTI from Doppler images, we developed a 2-step method. The Doppler spectrum was first automatically split into segments, each corresponding to a cardiac cycle. A deep-learning model then traced the modal velocity curve in each segment. The areas under the tracings were averaged to obtain the final VTI estimate.

### Velocity peak extractor

Before splitting the Doppler spectrum, the portion of the spectrum corresponding to motion away from the sensor was automatically cropped using data in the image header (Fig. 1). Heartbeat data overlapping the spectrum were automatically blackened using a colour filter. The resulting spectrum was converted to greyscale.

To identify velocity curves corresponding to each cardiac cycle, a band of velocities between one-fourth and two-thirds of the maximum velocity was examined (Fig. 1B). Within this band, columns of pixels with average intensity greater than the average of the band were marked as potentially overlapping velocity peaks. Contiguous marked columns were grouped to form initial guesses of the time ranges corresponding to velocity peaks. For a given image, time ranges shorter than 80% of the length of the longest time range were dropped. The remaining time ranges were padded to prevent the removal of peak edges.

**Table 1.** Characteristics of subjects in the training, validation, and test sets

| | Training | Validation | Test | Total | *P* value |
|---|---|---|---|---|---|
| Has 5Ch video | 195 | 32 | 32 | 259 | — |
| Has Doppler | 162 | 29 | 28 | 219 | — |
| Has 5Ch video & Doppler | 161 | 29 | 28 | 218 | — |
| Dilated cardiomyopathy | 47 (24.0) | 5 (15.6) | 4 (12.5) | 56 (21.5) | 0.24 |
| Male | 105 (53.6) [1] | 17 (53.1) | 16 (50.0) | 138 (53.1) [1] | 0.92 |
| Age (y) | 7.23 (3.04-11.35) [1] | 7.07 (3.99-13.05) | 10.42 (4.98-13.80) | 7.42 (3.24-12.66) [1] | 0.19 |
| Weight (kg) | 27.5 (18.5-39.7) [47] | 29.1 (17.8-48.8) [5] | 41.0 (21.6-53.4) [4] | 28.8 (18.6-46.3) [56] | 0.21 |
| Height (cm) | 130 (107-152) [47] | 131 (106-155) [5] | 148 (114-161) [4] | 131 (108-157) [56] | 0.28 |
| Body mass index (kg/m$^2$) | 16.8 (15.6-18.6) [47] | 17.2 (15.3-20.3) [5] | 17.9 (16.2-20.8) [4] | 17.1 (15.6-19.2) [56] | 0.26 |
| Body surface area (m$^2$) | 0.95 (0.63-1.28) [2] | 0.97 (0.66-1.32) | 1.25 (0.78-1.54) | 0.95 (0.65-1.34) [2] | 0.14 |
| Heart rate (bpm) | 83 (70-104) [30] | 82 (69-97) [2] | 77 (68-87) [3] | 82 (70-102) [35] | 0.40 |
| LVOT diameter (mm) | 15.2 (12.1-17.7) [1] | 16.0 (13.5-17.8) | 15.6 (13.4-19.5) | 15.5 (12.7-18.0) [1] | 0.30 |
| VTI (cm) | 19.4 (15.6-22.6) [34] | 19.5 (15.6-22.7) [3] | 21.7 (19.1-23.2) [4] | 19.6 (15.7-22.8) [41] | 0.04 |
| CO (L/min) | 3.05 (2.07-3.85) [35] | 2.98 (2.27-4.39) [3] | 3.43 (2.58-4.27) [4] | 3.09 (2.18-3.93) [42] | 0.15 |
| CI (L/min/m$^2$) | 3.01 (2.51-3.61) [36] | 3.14 (2.67-3.82) [3] | 3.13 (2.62-3.61) [4] | 3.06 (2.52-3.67) [43] | 0.90 |

Values are reported as number (%) or median (interquartile range), with the number of missing data points given in square brackets.
The *P* values compare the training, validation, and test sets using the analysis of variance.
5Ch, 5-chamber view; CI, cardiac index; CO, cardiac output; LVOT, left ventricular outflow tract; VTI, velocity time integral.

The spectrum was split into segments defined by the time ranges, each intended to correspond to a cardiac cycle.

## Modal velocity curve-tracing model

Each spectrum segment was input to a convolutional neural network model based on the ResNet-18 architecture.[25] The model consists of a sequence of 2D convolutional layers, which extract increasingly complex image features. A fully connected layer combines these features and outputs a vector of velocities representing the estimated curve tracing. Negative velocity estimates were set to zero. Velocities were estimated in pixels and later converted to cm/s. For each subject, the areas under the estimated curves were averaged to obtain the final VTI estimate.

Before being input to the model, each spectrum segment was rescaled to the size of the largest segment, 417 × 286 pixels, and then normalized by subtracting the mean and dividing by the standard deviation of the segment.

The model was trained to minimize the MSE between the velocities in the estimated and expert-traced curves, using the AdamW algorithm.[26] Training hyperparameters were selected by sequential model-based optimization using tree-structured Parzen estimators.[24] Additional details of the training procedure are given in the Supplemental Materials.

## Model evaluation

For each model, we computed the root MSE (RMSE), mean absolute error (MAE), mean absolute percentage error (MAPE), and coefficient of determination ($R^2$) between the estimated and actual values for each subject group. To evaluate clinical applicability, we performed the Bland-Altman analysis of each model in the test set, comparing estimated values with those of the primary expert rater (C.S.). The Bland-Altman analysis was also used to assess inter-rater

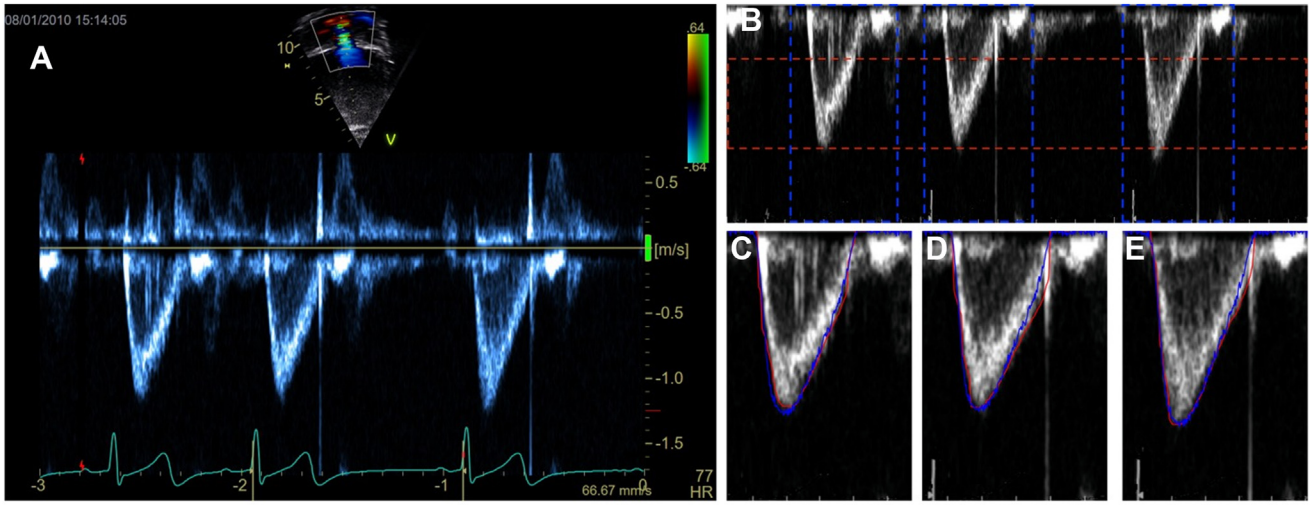


**Figure 1.** Velocity peak extraction and modal velocity curve tracing. The original Doppler image (A) was cropped below the horizonal axis (B). In (B), the region outlined in red is the portion of the Doppler spectrum in which the average intensities of columns of pixels were used to locate the velocity peaks; the regions outlined in blue are the spectrum segments identified by the velocity peak extractor. (C-E) depict the expert rater's tracing (red) and model-calculated tracing (blue) of the modal velocity curve for each extracted cardiac cycle.

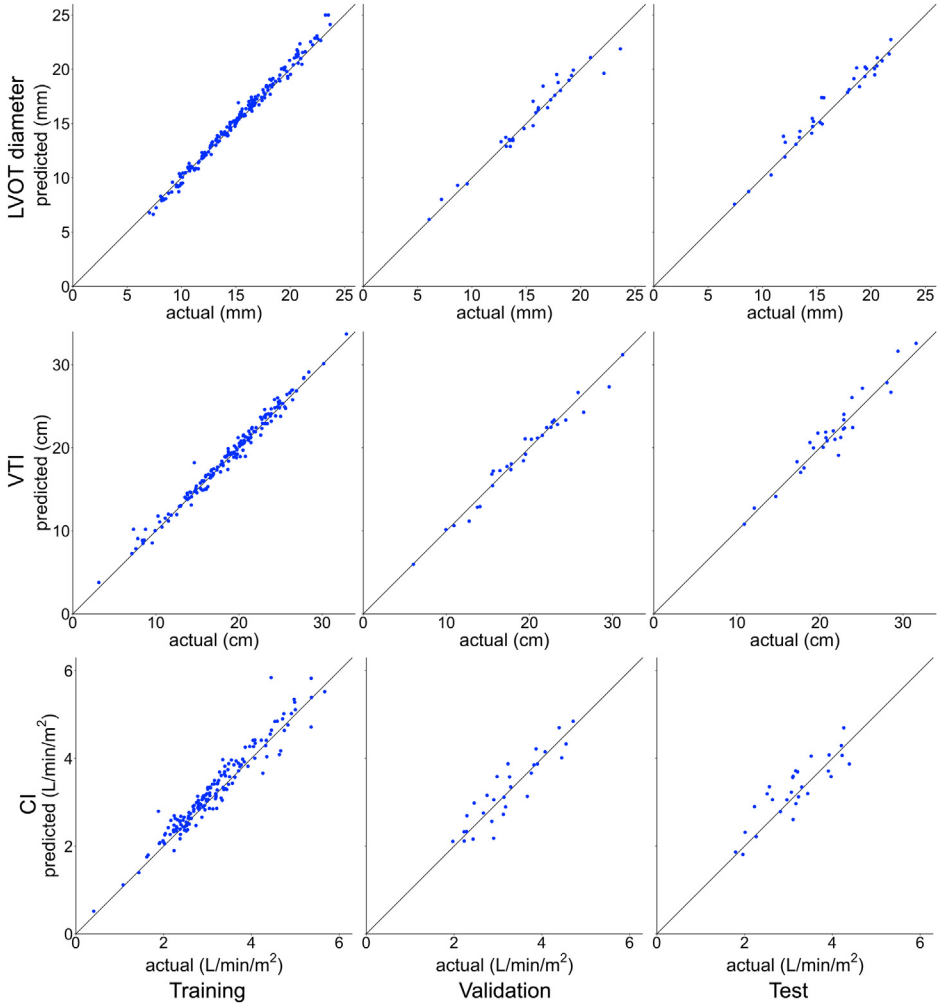


**Figure 2.** Estimated vs actual values of left ventricular outflow tract diameter, velocity time integral, and cardiac index in the training, validation, and test sets.

reliability of VTI measurement, comparing the 2 expert raters' measurements in the test set.

## Results

We found no significant differences in subject characteristics or cardiac metrics between the training, validation, and test sets, except VTI ($P = 0.04$), with the test set having larger values than the training and validation sets (Table 1).

For each model and subject group, we compared estimated and actual values in Figure 2. Performance metrics are summarized in Table 2, and the Bland-Altman analysis results are shown in Figure 3. In the test set, CO was calculated with the RMSE of 0.503 L/min, MAE of 0.382 L/min, MAPE of 10.8%, and $R^2$ of 0.909; CI was calculated with the RMSE of 0.389 L/min/m$^2$, MAE of 0.321 L/min/m$^2$, MAPE of 10.8%, and $R^2$ of 0.755. The Bland-Altman analysis showed that, in the test set, the LVOT diameter was predicted with a bias of +0.32 mm and 95% limits of agreement from -1.13 to 1.77 mm; VTI was predicted with a bias of +0.20 cm and 95% limits of agreement from -2.38 to 2.77 cm; and CI was predicted with a bias of +0.14 L/min/m$^2$ and 95% limits of agreement from -0.58 to 0.86 L/min/m$^2$ (Fig. 3).

The secondary expert rater evaluated VTI in 26 of the 28 test subjects. The Bland-Altman analysis comparing the 2 raters' measurements showed a bias of 0.49 cm and 95% limits of agreement from -1.97 to 2.95 cm. This inter-rater bias is greater than that between our model and the primary expert rater, and the 95% limits of agreement are of similar size (4.92 cm between raters and 5.15 cm in our model).

An example of the velocity peaks detected by the peak extractor is shown in Figure 1. The peak extractor identified 896 spectrum segments. From the original Doppler spectra, the expert selected 594 peaks for tracing. Of the expert-selected peaks, 16 were not automatically identified by the velocity peak extractor. In no case did the velocity peak extractor identify a spectrum segment whose boundaries overlapped the expert's tracing.

## Discussion

Our model automatically estimates CO with a very strong correlation and a bias of 0.17 L/min. The MAPE of 10.8%

**Table 2.** Performance metrics for models predicting the LVOT diameter, VTI, CO, and CI in the training, validation, and test sets

| | Training | Validation | Test |
|---|---|---|---|
| LVOT diameter | | | |
| RMSE (mm) | 0.474 | 0.848 | 0.795 |
| MAE (mm) | 0.370 | 0.574 | 0.588 |
| MAPE (%) | 2.52 | 3.70 | 3.80 |
| $R^2$ | 0.991 | 0.954 | 0.964 |
| VTI | | | |
| RMSE (cm) | 0.719 | 0.959 | 1.31 |
| MAE (cm) | 0.529 | 0.725 | 1.06 |
| MAPE (%) | 3.29 | 3.93 | 4.85 |
| $R^2$ | 0.982 | 0.972 | 0.930 |
| CO | | | |
| RMSE (L/min) | 0.308 | 0.363 | 0.503 |
| MAE (L/min) | 0.199 | 0.263 | 0.382 |
| MAPE (%) | 6.81 | 8.80 | 10.8 |
| $R^2$ | 0.971 | 0.928 | 0.909 |
| CI | | | |
| RMSE (L/min/m$^2$) | 0.266 | 0.336 | 0.389 |
| MAE (L/min/m$^2$) | 0.204 | 0.269 | 0.321 |
| MAPE (%) | 6.81 | 8.80 | 10.8 |
| $R^2$ | 0.932 | 0.823 | 0.755 |

CI, cardiac index; CO, cardiac output; LVOT, left ventricular outflow tract; MAE, mean absolute error; MAPE, mean average percentage error; $R^2$, coefficient of determination; RMSE, root-mean-squared error; VTI, velocity time integral.

surpasses conventionally acceptable accuracy for clinical CO measurement in paediatrics.[20,27] The consistency between our VTI model and expert measurement is comparable with the consistency between expert raters. The LVOT diameter, VTI, and combined CO models performed well over broad ranges of their respective metrics, without noticeably larger inaccuracy at extreme values. Although subjects in the test set had larger VTI and CO values than the training set, the accuracy of the models in the test set suggests robustness rather than a bias toward training data trends. The performance of the LVOT diameter model (MAPE 3.80%) was similar to that of the VTI model (MAPE 4.85%). However, as CO is proportional to the product of VTI and the square of the LVOT diameter, it is likely that much of the inaccuracy of the combined CO model was due to inaccuracy in the LVOT diameter estimation.

The combination of our VTI and LVOT diameter models enables rapid automatic estimation of CO. The combined model is advantageous as it can be applied to various ultrasound devices without relying on manufacturer- or model-specific proprietary software and can be used on basic computers rather than being tied to ultrasound machines. However, because most of the images in this study were acquired on the same ultrasound model, further study is needed to verify our model's performance on other ultrasound machines. The model can be used to analyse previously acquired echocardiographic data without access to the original hardware. The deep-learning approaches allow the models to exploit complex spatial and temporal features in the image data, without the need to explicitly define them beforehand. By retraining existing deep-learning models, we developed accurate models using much smaller datasets than are typically required when starting from random initial model parameters. This has major implications for other applications in paediatrics, in which large patient data sets are difficult to acquire and few paediatric deep-learning models exist.

Although the Fick principle is considered the gold standard of CO measurement, it is a difficult technique for clinical use, especially in paediatrics. Although considered a reference technique, it has important limitations, as it requires estimation of oxygen consumption, which is very difficult to directly measure. Oxygen-consumption data are typically based on the Lafarge method, which is inaccurate in paediatrics.[28,29] Thermodilution catheters may be too large for paediatric use, require catheter manipulation, and are not generally used in routine clinical practice.[30] Transpulmonary techniques, such as PiCCO (Pulsion Medical Systems, Munich, Germany), are less invasive, validated methods, correlating well with Fick in paediatrics.[31] However, the requirement for an internal jugular venous central line and a 4 F femoral arterial catheter limits its use in practice and is often restricted to intensive care units.[32] Echocardiography offers a noninvasive,

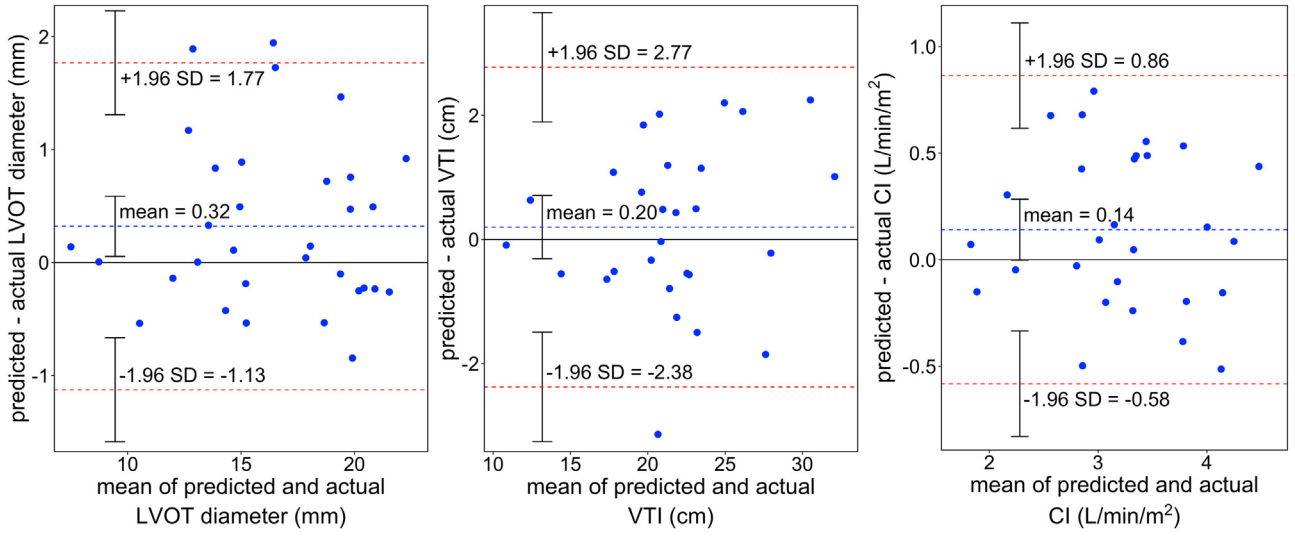


**Figure 3.** Bland-Altman plots of the left ventricular outflow tract (LVOT) diameter, velocity time integral (VTI), and cardiac index (CI) model calculation in the test set. SD, standard deviation.

readily available bedside measurement of CO[33] but requires expertise in image acquisition and interpretation. Accurate measurement of the LVOT diameter is critical, as its value is squared when computing CO, increasing the impact of its measurement error. Doppler-based measurements have been validated against the Fick principle.[20] Paediatric CO measurement using Doppler has an intraobserver repeatability of 2.1-22% and an interobserver repeatability of 3.1-21.7%.[20] The mean percentage error of ±30% in CO estimation is acceptable for clinicians.[18,34]

In adult practice, LVOT VTI, alone, is regularly used to estimate stroke volume,[35] as the LVOT diameter remains constant over time. The American Society of Echocardiography recognizes a normal VTI >18 cm for monitoring CO therapeutic interventions in adults.[36] In healthy children, normal values for the LVOT diameter and VTI vary with age and body surface area, necessitating individual patient calculation to avoid overdiagnosing low-CO states,[37,38] but monitoring LVOT VTI can be a useful alternative monitor of left ventricular performance in children >1 year of age.[39] Our future work includes developing a model to identify the most appropriate images to measure the LVOT diameter and VTI.

### Limitations

This model was tested on a small group of patients who reflect extremes of CO. Further modifications using intermediate reductions in CO are warranted. However, we are encouraged by the consistency of our predictions, suggesting likely generalization beyond the observations we tested. As our model was tested on images acquired by experts, further testing on images acquired by nonexperts would improve generalizability of the model to high-impact areas of use, enabling greater utilization of ECHO across specialties. Model generalizability could also be improved using images acquired from different ECHO machines and different patient populations and pathologies.

The potential benefits of this model include supporting clinicians in real-time bedside calculation of CO, identification of low-CO states, and response to treatment. This model may reduce operator error in the identification of the LVOT diameter and VTI, and provide confirmation before instigating treatment to modify CO. This is especially important in patients for whom CO is difficult to measure accurately, or in clinical areas where expert paediatric cardiology support may not be available, such as operating rooms or emergency departments. In paediatric emergency medicine, this might include the treatment of systemic sepsis. In paediatric anaesthesia, this might include cases where hypotension and/or the circulating volume might be difficult to estimate and the treatment might include fluids, pressors and/or inotropes. Examples include neonatal laparotomies, renal transplantation recipients, or surgery for burn patient populations in which there is a greater likelihood of harm from incorrect treatment. Future work will test our model in these situations, to assess its utility in clinical decision-making.

## Ethics Statement

This research has adhered to the ethical guidelines mandated by the Research Ethics Board at The Hospital for Sick Children, Toronto, Canada.

## Funding Sources

This work was supported by The Hospital for Sick Children, Perioperative Services Facilitator Grant Program and the Canadian Centre for Computational Genomics (C3G), part of the Genome Technology Platform (GTP), funded by Genome Canada through Genome Quebec and Ontario Genomics. The funding/sponsors did not participate in study design, collection analysis or interpretation of this data, the writing of this report or the decision to submit this paper for publication.

## Disclosures

The authors have no conflicts of interest to disclose.

## Author Contributions

S.U. performed the statistical analysis, developed the VTI model, trained, tested, and validated the model, prepared the manuscript including the tables and figures, and reviewed the final manuscript. M.Z. collected and analysed the data, prepared the manuscript, and reviewed the final manuscript. L.E. performed the statistical analysis, manuscript preparation, and reviewed the final manuscript. C.S. collected and analysed the data and critically reviewed the manuscript for important intellectual content and reviewed the final manuscript. L.M. provided advice regarding study implementation, assisted in manuscript preparation, provided critical intellectual content, and reviewed the final manuscript. K.T. conceived the study, wrote the REB protocol, implemented the study, analysed the data, literature search, and wrote the final manuscript. All authors approved the final manuscript as submitted and agree to be accountable for all aspects of the work.

## References

1. Egan J, Festa M, Cole AD, et al. Clinical assessment of cardiac performance in infants and children following cardiac surgery. *Intensive Care Med*. 2005;31:568−573.

2. Bhananker SM, Ramamoorthy C, Geiduschek JM, et al. Anesthesia-related cardiac arrest in children: update from the Pediatric Perioperative Cardiac Arrest Registry. *Anesth Analg*. 2007;105:344−350.

3. Ramamoorthy C, Haberkern CM, Bhananker SM, et al. Anesthesia-related cardiac arrest in children with heart disease: data from the Pediatric Perioperative Cardiac Arrest (POCA) Registry. *Anesth Analg*. 2010;110:1376−1382.

4. Wakeling HG, McFall MR, Jenkins CS, et al. Intraoperative oesophageal Doppler guided fluid management shortens postoperative hospital stay after major bowel surgery. *Br J Anaesth*. 2005;95:634−642.

5. Carcillo JA, Fields AI. Clinical practice parameters for hemodynamic support of pediatric and neonatal patients in septic shock. *Crit Care Med*. 2002;30:1365−1378.

6. Rivers EP, Ahrens T. Improving outcomes for severe sepsis and septic shock: tools for early identification of at-risk patients and treatment protocol implementation. *Crit Care Clin*. 2008;24(suppl):S1−S47.

7. Taylor K, Kim WT, Maharramova M, et al. Intraoperative management and early postoperative outcomes of pediatric renal transplants. *Paediatr Anaesth*. 2016;26:987−991.

8. Marik PE, Lemson J. Fluid responsiveness: an evolution of our understanding. *Br J Anaesth*. 2014;112:617–620.

9. Holte K, Sharrock NE, Kehlet H. Pathophysiology and clinical implications of perioperative fluid excess. *Br J Anaesth*. 2002;89:622–632.

10. Sakka SG, Klein M, Reinhart K, Meier-Hellmann A. Prognostic value of extravascular lung water in critically ill patients. *Chest*. 2002;122:2080–2086.

11. Chung FT, Lin SM, Lin SY, Lin HC. Impact of extravascular lung water index on outcomes of severe sepsis patients in a medical intensive care unit. *Respir Med*. 2008;102:956–961.

12. Gan H, Cannesson M, Chandler JR, Ansermino JM. Predicting fluid responsiveness in children: a systematic review. *Anesth Analg*. 2013;117:1380–1392.

13. Raux O, Spencer A, Fesseau R, et al. Intraoperative use of transoesophageal Doppler to predict response to volume expansion in infants and neonates. *Br J Anaesth*. 2012;108:100–107.

14. Saugel B, Thiele RH, Hapfelmeier A, Cannesson M. Technological assessment and objective evaluation of minimally invasive and noninvasive cardiac output monitoring systems. *Anesthesiology*. 2020;133:921–928.

15. O'Neill R, Dempsey EM, Garvey AA, Schwarz CE. Non-invasive cardiac output monitoring in neonates. *Front Pediatr*. 2021;8, 614585.

16. Nguyen HB, Banta DP, Stewart G, et al. Cardiac index measurements by transcutaneous Doppler ultrasound and transthoracic echocardiography in adult and pediatric emergency patients. *J Clin Monit Comput*. 2010;24:237–247.

17. Karlsson J, Svedmyr A, Wiegele M, et al. Cardiac output assessments in anesthetized children: dynamic capnography versus esophageal Doppler. *Anesth Analg*. 2022;134:644–652.

18. Critchley LAH, Critchley AAJH. A meta-analysis of studies using bias and precision statistics to compare cardiac output measurement techniques. *J Clin Monit Comput*. 1999;15:85–91.

19. Klugman D, Berger JT. Echocardiography as a hemodynamic monitor in critically ill children. *Pediatr Crit Care Med*. 2011;12(suppl):S50–S54.

20. Chew MS, Poelaert J. Accuracy and repeatability of pediatric cardiac output measurement using Doppler: 20-year review of the literature. *Intensive Care Med*. 2003;29:1889–1894.

21. Ouyang D, He B, Ghorbani A, et al. Video-based AI for beat-to-beat assessment of cardiac function. *Nature*. 2020;580:252–256.

22. Tran D, Wang H, Torresani L, et al. A closer look at spatiotemporal convolutions for action recognition. arXiv:1711.11248v3 2018

23. Kingma DP, Ba J. Adam: A Method for Stochastic Optimization, CoRR abs/1412.6980, 2015.

24. Bergstra J, Bardenet Rm, Bengio Y, Kégl B. In: Shawe-Taylor J, Zemel R, Bartlett P, Pereira F, Weinberger KQ, eds. *Algorithms for hyper-parameter optimization*. 2011.

25. He K, Zhang X, Ren S, Sun J. *Deep residual learning for image recognition, 2016 IEEE COnference on Computer Vision and Pattern Recognition (CVPR)*. 2016:770–778.

26. Loshchilov I, Hutter F. Decoupled weight decay regularization. arXiv: 1711.05101 2017

27. Levy RJ, Chiavacci RM, Nicolson SC, et al. An evaluation of a noninvasive cardiac output measurement using partial carbon dioxide rebreathing in children. *Anesth Analg*. 2004;99:1642–1647.

28. Rutledge J, Bush A, Shekerdemian L, et al. Validity of the LaFarge equation for estimation of oxygen consumption in ventilated children with congenital heart disease younger than 3 years—a revisit. *Am Heart J*. 2010;160:109–114.

29. Limón A, Escribá FJ, Ferrari V, Monzó-Fabuel S, Argente P. The inaccuracy of LaFarge equations estimating the oxygen consumption in children under 3 years age. *Rev Esp Anestesiol Reanim (Engl Ed)*. 2019;66:467–473.

30. Lemson J, Nusmeier A, van der Hoeven JG, Lehman R, Ceccheti C. The pulmonary artery catheter in the pediatric intensive care unit: not the way to go. *Pediatr Crit Care Med*. 2012;13:250–251.

31. Pauli C, Fakler U, Genz T, et al. Cardiac output determination in children: equivalence of the transpulmonary thermodilution method to the direct Fick principle. *Intensive Care Med*. 2002;28:947–952.

32. Proulx F, Lemson J, Choker G, Tibby SM. Hemodynamic monitoring by transpulmonary thermodilution and pulse contour analysis in critically ill children. *Pediatr Crit Care Med*. 2011;12:459–466.

33. Quiñones MA, Otto CM, Stoddard M, Waggoner A, Zoghbi WA. Recommendations for quantification of Doppler echocardiography: a report from the Doppler Quantification Task Force of the Nomenclature and Standards Committee of the American Society of Echocardiography. *J Am Soc Echocardiogr*. 2002;15:167–184.

34. Odor PM, Bampoe S, Cecconi M. Cardiac output monitoring: validation studies-how results should be presented. *Curr Anesthesiol Rep*. 2017;7:410–415.

35. Cecconi M, De Backer D, Antonelli M, et al. Consensus on circulatory shock and hemodynamic monitoring. Task Force of the European Society of Intensive Care Medicine. *Intensive Care Med*. 2014;40:1795–1815.

36. Porter TR, Shillcutt SK, Adams MS, et al. Guidelines for the use of echocardiography as a monitor for therapeutic intervention in adults: a report from the American Society of Echocardiography. *J Am Soc Echocardiogr*. 2015;28:40–56.

37. Pees C, Glagau E, Hauser J, Michel-Behnke I. Reference values of aortic flow velocity integral in 1193 healthy infants, children, and adolescents to quickly estimate cardiac stroke volume. *Pediatr Cardiol*. 2013;34:1194–1200.

38. Díaz A, Zócalo Y, Cabrera-Fischer E, Bia D. Reference intervals and percentile curve for left ventricular outflow tract (LVOT), velocity time integral (VTI), and LVOT-VTI-derived hemodynamic parameters in healthy children and adolescents: analysis of echocardiographic methods association and agreement. *Echocardiography*. 2018;35:2014–2034.

39. Navaratnam M, Punn R, Ramamoorthy C, Tacy TA. LVOT-VTI is a useful indicator of low ventricular function in young patients. *Pediatr Cardiol*. 2017;38:1148–1154.

## Supplementary Material

To access the supplementary material accompanying this article, visit *CJC Pediatric and Congenital Heart Disease* at https://www.cjcpc.ca// and at https://doi.org/10.1016/j.cjcpc.2022.11.001